PHYSICS AND CHEMISTRY OF SOLID STATE
V. 22, No. 1 (2021) pp. 39-44
Section: Chemistry

DOI: 10.15330/pcss.22.1.39-44

Vasyl Stefanyk Precarpathian National University

ФІЗИКА І ХІМІЯ ТВЕРДОГО ТІЛА
Т. 22, № 1 (2021) С. 39-44
Хімічні науки

UDC: 546.712'24'86 ISSN 1729-4428

E.N. Orujlu[1], Z.S. Aliev[2,3], I.R. Amiraslanov[3], M.B. Babanly[1]

Phase Equilibria of the MnTe-Sb_2Te_3 System and Synthesis of Novel Ternary Layered Compound – $MnSb_4Te_7$

[1]*Institute Catalysis and Inorganic Chemistry, ANAS, Baku, Azerbaijan, elnur.oruclu@yahoo.com*
[2]*Azerbaijan State Oil and Industry University, Baku, Azerbaijan, ziyasaliev@gmail.com*
[3]*Institute of Physics, ANAS, Baku, Azerbaijan, iamiraslan@gmail.com*

By using Differential Thermal Analysis (DTA) and Powder X-ray Diffraction (PXRD) techniques, the phase diagram of the MnTe-Sb_2Te_3 system has been constructed for the first time in the entire composition range. The system features two ternary layered van der Waals (vdW) compounds. Apart from known $MnSb_2Te_4$, novel $MnSb_4Te_7$ which a structural analogous of the known $MnBi_4Te_7$ was found in the system. Crystal structure parameters of both compounds were determined by Rietveld refinement using the fundamental parameter approach. Both compounds were found to decompose via peritectic reactions and possess significant homogeneity ranges. The title system is also characterized by the existence of the wide solid solution field based on the starting Sb_2Te_3. The present results would be useful for the bulk single crystal growth of both compounds from the liquid phase via the determination of primary crystallization areas.

Keywords: MnTe-Sb_2Te_3 system; manganese antimony tellurides; magnetic topological insulators; X-ray diffraction; phase diagram.

Received 25 January 2021; Accepted 10 February 2021.

Introduction

VdW materials based on bismuth and antimony chalcogenides have received great interest thanks to the attractive combination of intriguing thermoelectric and topological insulator (Tl) properties [1-4]. Non-trivial band topology and complex structures of these materials allow for the realization of many novel topological phenomena, such as quantum Hall effect, quantum spin Hall effect, quantum anomalous Hall effect (QAHE), Majorana fermions, topological axion insulators, magnetoresistance switch effect, etc., which have huge potential for electronic, spintronic applications or other future technologies [5-12].

The most recent research topic in this field concerns materials having both magnetic and topological features. Breaking time-reversal symmetry and open an exchange gap in the Dirac surface states in Tls are key points for the realization of magnetism [13-16]. Results of doping trivial Tl materials with magnetic transition metals by Molecular Beam Epitaxy and Bridgman methods show magnetic ordering at extremely low temperatures which is the main factor that prevents its practical use [17-20]. However, layered heterostructures contain both magnetic and Tl layers succeed to integrate these seemingly incompatible characters [15, 16, 21], e.g., recently confirmed first intrinsic antiferromagnetic TI - $MnBi_2Te_4$ [22]. In this connection, other possible ternary compounds containing magnetic transition metals (*M*) – V, Cr, Mn, and Fe in both *M*Te–Sb_2Te_3 and *M*Te–Bi_2Te_3 systems are believed to be an ideal platform to explore interesting topological quantum effects that remains elusive experimentally so far.

The phase diagram of the MnTe-Bi_2Te_3 quasi-binary system was investigated [23]. The system contains three ternary compounds that melt incongruently via peritectic reactions and further research revealed the existence of other homologues series [23-25]. It was also revealed that interlayer antiferromagnetic ordering weakens from $MnBi_2Te_4$ to $MnBi_6Te_{10}$ which is ferromagnetic and furtherly disappears in high members of homologues

series [25]. The temperature-dependent changes in the electronic structure of the $MnBi_2Te_4$ were studied in [26].

To our best knowledge, the phase diagram of the MnTe-Sb_2Te_3 binary system is not yet available in the literature. Crystal structure determination and some theoretical studies devoted to electronic structure, magnetism, etc., of the $MnSb_2Te_4$ are reported in [27-32]. The observable antiferromagnetic ordering temperature for $MnSb_2Te_4$ (19 K [28]) is lower comparing to $MnBi_2Te_4$ (24 K [22]).

In the present work, the phase diagram of the MnTe-Sb_2Te_3 binary system is determined experimentally for the first time and crystal structure refinement of ternary compounds is presented.

The boundary binary compounds of the system have been investigated on several occasions [33-37]. MnTe melts peritectically at 1155 ± 5 °C and crystallizes in the hexagonal crystal structure, space group *P*63/*mmc* (no. 194) with unit cell parameters a = 4.1429 Å, c = 6.7076 Å [35]. Hexagonal NiAs-type crystal structure undergo several phase transformations. Sb_2Te_3 melts peritectically at 620 °C and crystallizes in a rhombohedral unit cell having the lattice constants a = 4.264 Å; c = 30.458 Å (space group, *R*-3*m* (no. 166)) [36, 37].

I. Experimental details

High purity elemental components (99.9999 %, Alfa Aesar and Sigma-Aldrich) were used to synthesize binary starting compounds MnTe and Sb_2Te_3. Mixture of components inside the vacuum (~10^{-3} Pa residual pressure) sealed quartz ampoules were melted at 1250 °C and 700 °C, respectively. Glassy carbon crucibles were used to synthesize MnTe to prevent manganese reaction with quartz. Both binary compounds were analyzed by DTA and PXRD to check the phase purity and results were close to the values reported in the literature [33-37]. DTA examination of MnTe shows four endothermic peaks at the temperatures 955, 1020, 1055, and 1151 °C, respectively. The first three peaks belong to polymorphic transformations, while the last one indicates the peritectic decomposition temperature of MnTe.

Samples of MnTe-Sb_2Te_3 system having different stoichiometric compositions were prepared from pre-synthesized binary compounds in the evacuated sealed quartz ampoules. The total weight of each sample was 1 g. All samples were heated up to 850 °C for 5h followed by quenching in icy-water. The obtained polycrystalline bulk samples annealed at 450 °C for 8 weeks to reach an equilibrium state.

All homogenized samples were examined by DTA and PXRD techniques. DTA spectrums were recorded on the LINSEIS HDSC PT1600 system (precision ±2 °C) with a heating rate of 10 °C/min from room temperature up to 1200 °C. Temperatures of thermal effects were taken mainly from heating curves. The PXRD patterns were obtained on a Bruker D2 PHASER diffractometer at room temperature using CuK_α radiation within $2\theta = 5^o \div 75^o$. Rietveld refinement using the fundamental parameter approach was performed with Fullprof software and graphics of structures were made using Vesta software.

II. Results and discussion

To identify phase equilibria in the MnTe-Sb_2Te_3 system over the entire concentration range, fourteen alloys were prepared. Fig. 1 shows the PXRD results of some selected alloys. The diffraction peaks of different phases can be identified by referring to the ICDD and COD databases. Characteristic peaks of different phases are described by different symbols. As can be seen from Fig. 1,*a*, an alloy having 90 mol% Sb_2Te_3 has similar reflection lines with a negligible shifting compared to pure Sb_2Te_3. This fact clearly confirms the existence of a solubility field based on Sb_2Te_3 about 11 - 12 mol%. In Fig. 1,*b*, the PXRD peaks of alloy 75 mol% Sb_2Te_3 indicate that, besides Sb_2Te_3, there is another phase that is not indexed by the database. Clearly distinguishable peaks at low angles allow us to assume that they more likely correspond to the $MnSb_4Te_7$ layered compound which is formed in similar $A^{IV}Te$-Sb_2Te_3 systems (A^{IV}–Ge, Sn, Pb). Since these two ternary compounds can be easily distinguished in XRD analysis with their characteristic non-overlapping peaks at small angles. In addition, analyzing the PXRD patterns of the equilibrated alloy correspond to the $MnSb_4Te_7$ stoichiometric composition (66.7 mol% Sb_2Te_3) indicates the existence of a new ternary compound in the MnTe-Sb_2Te_3 system as well (Fig. 1,*c*). A similar result was also found for an alloy having 60 mol% Sb_2Te_3 which is located in the two-phase $MnSb_2Te_4$ + $MnSb_4Te_7$ region according to its stoichiometric composition (Fig. 1,d). The $MnSb_2Te_4$ ternary phase forms in 50 mol% Sb_2Te_3 composition as phase pure form without any traces of other phases (Fig. 1,*e*), while PXRD results for 40 mol% Sb_2Te_3 composition was found to be a biphasic mixture of MnTe + $MnSb_2Te_4$ as expected (Fig. 1,*f*). All these results strongly prove the existence of a new compound in the system with a stoichiometric ratio of 1:4:7 in addition to 1:2:4. However, we found no evidence for the existence of other ternary compounds in the Sb_2Te_3-rich region. We believe that the atomic size factor is a dominant structural feature that prevents the formation of more complex members of homologous series in this system. The existence of a wide solubility field based on Sb_2Te_3 indicates that Sb atoms are relatively easy to substitute Mn atoms up to a certain amount so that we can predict that both ternary compounds should have homogeneity fields.

The Rietveld refinement was done to reveal the crystal structure of both ternary compounds. All refinements showed very good fits. The observed and calculated data of the powder diffraction patterns are shown in Fig. 2 and results of the Rietveld structural refinement are listed in Table 1. The compound $MnSb_2Te_4$ has the same trigonal structure as $MnBi_2Te_4$ with crystal lattice parameters a = 4.2445 Å and c = 40.862 Å. For $MnSb_4Te_7$, all diffraction patterns are indexed in the trigonal structure with lattice parameters a = 4.2413 Å and c = 23.761 Å. We note that determined unit cell parameters of $MnSb_2Te_4$ are in good agreement

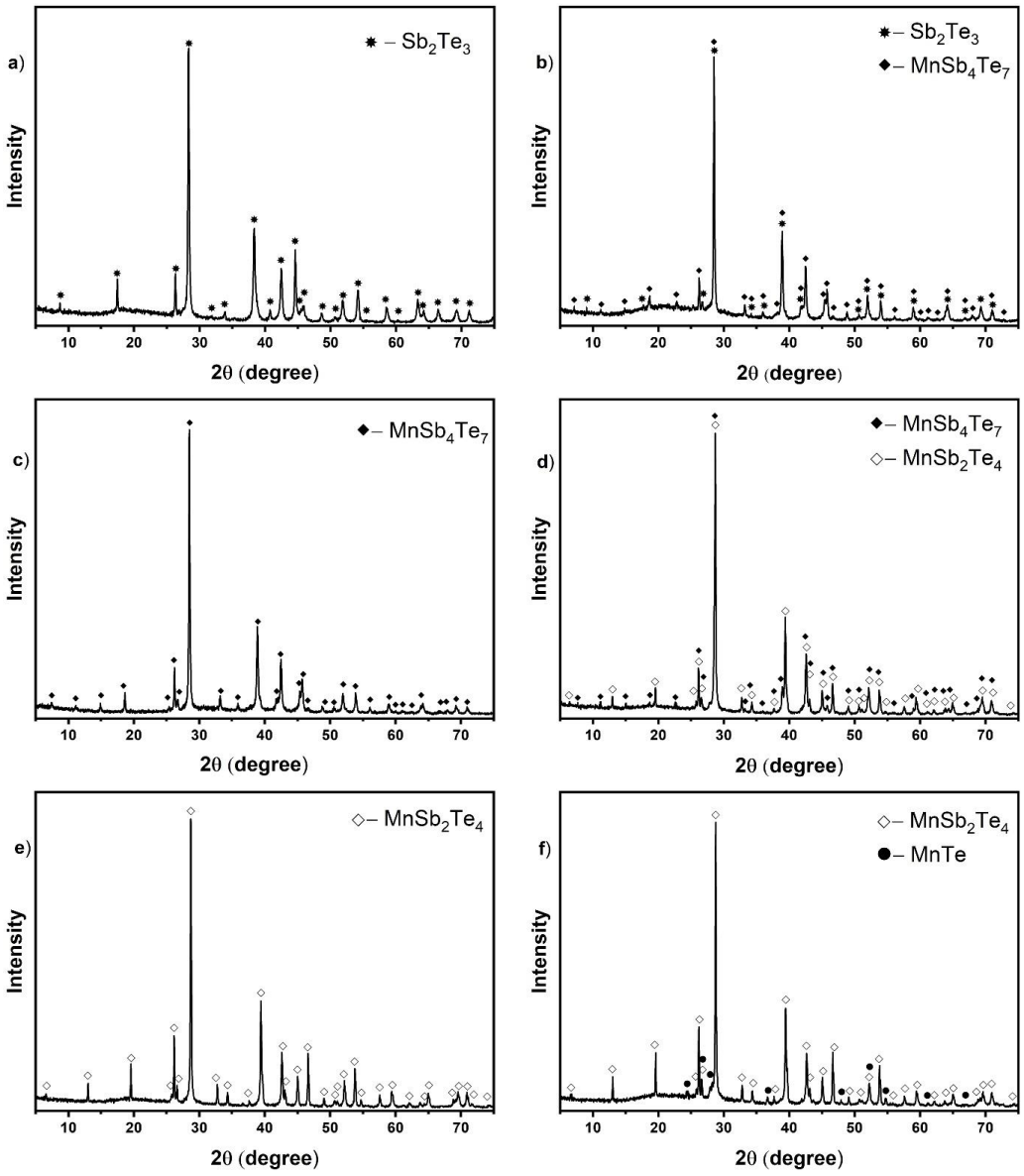

Fig. 1. PXRD patterns of some equilibrated alloys: a) 90 mol% Sb_2Te_3, b) 75 mol% Sb_2Te_3, c) 66.7 mol% Sb_2Te_3, d) 60 mol% Sb_2Te_3, e) 50 mol% Sb_2Te_3, c) 40 mol% Sb_2Te_3.

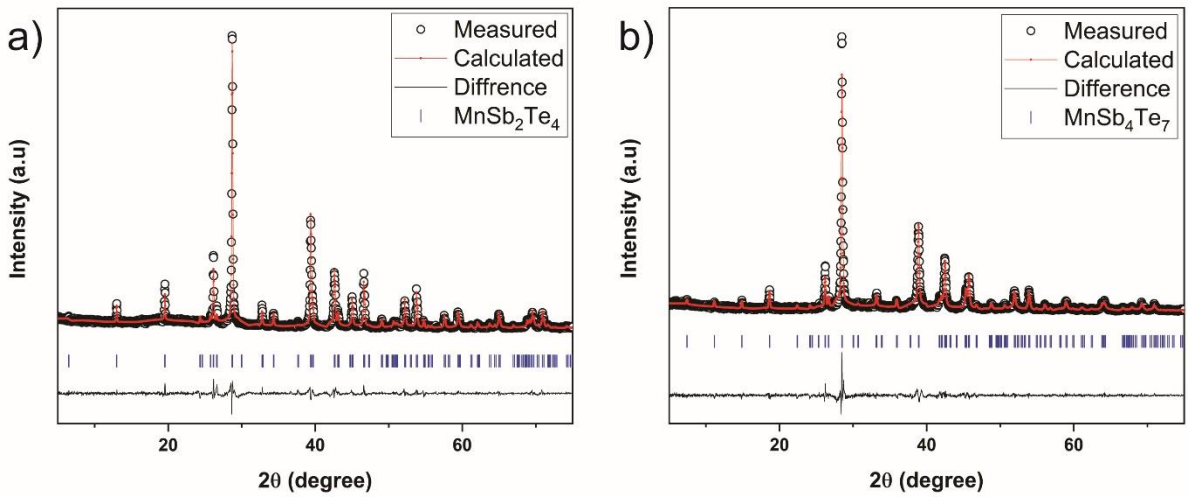

Fig. 2. Rietveld refinement profiles for the $MnSb_2Te_4$ (a) and $MnSb_4Te_7$ (b).

with already reported ones elsewhere in [27, 28]. However, the narrow homogeneity field of the $MnSb_2Te_4$ compound may cause some deviation from the values of the *a* and *c* parameters which suggests that other results can also be acceptable.

Both compounds exhibit tetradymite-type layered structure where unit cells consist of stacked septuple blocks of Te-Sb-Te-Mn-Te-Sb-Te for $MnSb_2Te_4$ (space group *R*-3*m*) and repetitions of the same septuple layer and quintuple layer blocks of Sb_2Te_3 for $MnSb_4Te_7$ (space group *P*-3*m*1) (Fig. 3). In each block, atomic layers are covalently bonded, whereas blocks itself connected via van der Waals interactions.

The phase diagram of the MnTe-Sb_2Te_3 (Fig. 4) system was constructed by means of DTA and PXRD results of annealed alloys. As can be seen from the figure, this system is a partial quasi-binary section of the

Table 1

Results of Rietveld refinements for the investigated phases

	$MnSb_2Te_4$	$MnSb_4Te_7$
Space group	*R*-3*m* (no. 166)	*P*-3*m*1 (no. 164)
Z	3	1
Temperature (K)	293	293
Unit cell parameter: *a* (Å)	4.2445(2)	4.2513(3)
c (Å)	40.862(3)	23.761(4)
Unit cell volume (Å^3)	637.534	371.9108
R_{Bragg}%	2.67	1.35
Radiation type	CuK$_\alpha$	CuK$_\alpha$

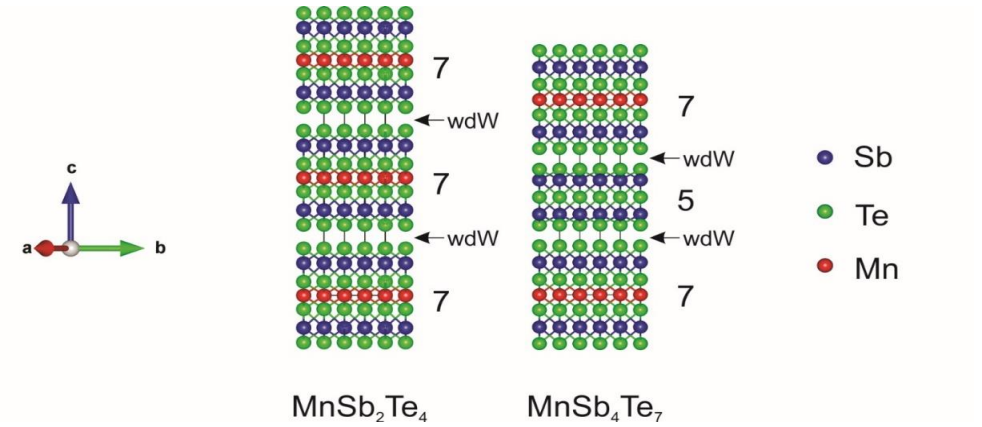

Fig. 3. Crystal structures of $MnSb_2Te_4$ and $MnSb_4Te_7$.

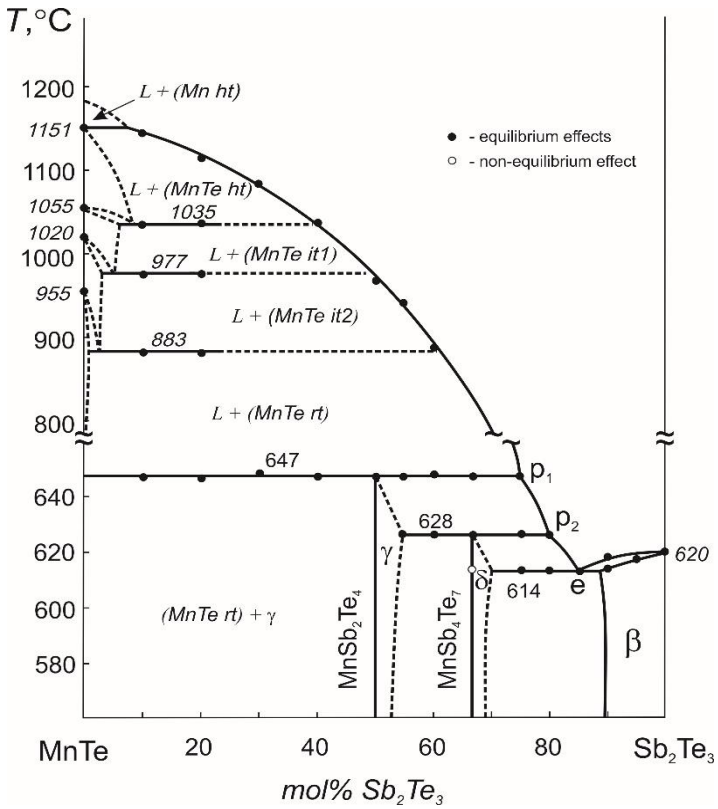

Fig. 4. Phase diagram of the MnTe-Sb_2Te_3 system.

Mn-Sb-Te system due to the incongruent melting character of manganese telluride. As discussed above, the MnTe-Sb_2Te_3 system host two ternary intermediate compounds. Both compounds melt by peritectic reactions:

$$L + MnTe\ rt \leftrightarrow MnSb_2Te_4\ (p_1, 647°C)$$

$$L + MnSb_2Te_4 \leftrightarrow MnSb_4Te_7\ (p_2, 628°C)$$

The composition of the invariant peritectic points corresponds to 75 (p_1) and 80 (p_2) mol% Sb_2Te_3, respectively. The system also has eutectic point (e) lies at 85 mol% Sb_2Te_3 and 614 °C. One can be seen from the phase diagram, both compounds possess significant homogeneity ranges. Besides, there is an approximately 11 - 12 mol% solubility region based on Sb_2Te_3. On the MnTe rich side, several polymorphic transformations were observed. By using DTA results, we determined that the temperatures of polymorphic transformations were significantly reduced compared to pure MnTe and occur by following metatectic reactions:

$$(MnTe\ ht) \leftrightarrow L+(MnTe\ it1)$$

$$(MnTe\ it1) \leftrightarrow L+(MnTe\ it2)$$

$$(MnTe\ it2) \leftrightarrow L+(MnTe\ rt)$$

The reaction temperatures were found to be 1035, 977, and 883 °C, respectively.

Conclusion

In this work, the phase relationship in the MnTe-Sb_2Te_3 system was determined and the phase diagram was constructed by using DTA and PXRD results of numerous equilibrated alloys. The system is characterized by the formation of two intermediate compounds, namely $MnSb_2Te_4$ and $MnSb_4Te_7$. Both compounds have a tetradymite-type layered structure and melt with peritectic reactions at 647 °C and 628 °C, respectively. There are significant solid-solubility fields based on both ternary compounds and starting Sb_2Te_3. The maximum solid-solubility of the Sb_2Te_3 is measured about 11 - 12 mol%.

Acknowledgments

The work has been carried out within the framework of the international joint research laboratory "Advanced Materials for Spintronics and Quantum Computing" (AMSQC) established between the Institute of Catalysis and Inorganic Chemistry of ANAS (Azerbaijan) and Donostia International Physics Center (Basque Country, Spain) and partially supported by the Science Development Foundation under the President of the Republic of Azerbaijan, a grant EİF/MQM/Elm-Tehsil-1-2016-1(26)-71/01/4-M-33.

Orujlu E.N. – Ph.D. student, junior researcher, 'Thermodynamics of inorganic functional compounds' laboratory of ICIC;
Aliev Z.S. – Ph.D., Associate Professor, ASOIU;
Amiraslanov I.R. – Professor, Institute of Physics ANAS;
Babanly M.B. – Professor, deputy-director of ICIC.

[1] L.L. Wang, D.D. Johnson, Phys. Rev. B 83(24), 241309 (2011) (https://doi.org/10.1103/PhysRevB.83.241309).
[2] H. Shi, et al., Phys. Rev. Applied 3, 014004 (2015) (https://doi.org/10.1103/PhysRevApplied.3.014004).
[3] B.Z. Rameshti, et al., Phys. Rev. B 94, 205401 (2016) (https://doi.org/10.1103/PhysRevB.94.205401).
[4] N. Xu, et al., npj Quant. Mater. 2, 51 (2017) (https://doi.org/10.1038/s41535-017-0054-3).
[5] W.Q. Zou, et al., Appl. Phys. Lett. 110, 212401 (2017) (http://doi.org/10.1063/1.4983684).
[6] X.-L. Qi, S.-C. Zhang, Phys. Today 63(1), 33 (2010) (https://doi.org/10.1063/1.3293411).
[7] K. He, et. al., Annu. Rev. Condens. Matter Phys. 9, 329 (2018) (https://doi.org/10.1146/annurev-conmatphys-033117-054144).
[8] Q. L. He, et al., Science 357, 294 (2017) (https://doi.org/10.1126/science.aag2792).
[9] Y. Hou, R. Wu, Nano Lett. 19, 2472 (2019) (https://doi.org/10.1021/acs.nanolett.9b00047).
[10] M. Mogi, et al., Nat. Mater. 16, 516 (2017) (https://doi.org/10.1038/nmat4855).
[11] H.B. Zhang, et al., Adv. Mater. 24, 132 (2012) (https://doi.org/10.1002/adma.201103530).
[12] J. Wang, et al., Nano Res. 5, 739 (2012) (https://doi.org/10.1007/s12274-012-0260-z).
[13] J. Wu, et al., Sci. Adv. 5(11), eaax9989 (2019) (https://doi.org/10.1126/sciadv.aax9989).
[14] Y. Tokura, et. al., Nat. Rev. Phys. 1, 126 (2019) (https://doi.org/10.1038/s42254-018-0011-5).
[15] R.S.K. Mong, J.E. Moore, Nature 576(7787), 390 (2019) (https://doi.org/10.1038/d41586-019-03831-7).
[16] V. Litvinov, Magnetism in Topological Insulators (Springer International Publishing, 2020).
[17] C.Z. Chang, et al., Science 340(6129), 167 (2013) (https://doi.org/10.1126/science.1234414).
[18] C. Z. Chang, et al., Nat. Mater. 14, 473 (2015) (https://doi.org/10.1038/nmat4204).
[19] J. Teng, et al., J. Semicond. 40(8), 081507 (2019) (https://doi.org/10.1088/1674-4926/40/8/081507).
[20] J. Ge, et al., Solid State Commun. 2011, 29 (2015) (https://doi.org/10.1016/j.ssc.2015.03.012).
[21] T. Hesjedal and Y. Chen. Nature Mater. 16, 3 (2017) (https://doi.org/10.1038/nmat4835).
[22] M.M. Otrokov, et al., Nature 576, 416 (2019) (https://doi.org/10.1038/s41586-019-1840-9).
[23] Z.S. Aliev, et al., J. Alloys Compd. 789, 443 (2019) (https://doi.org/10.1016/j.jallcom.2019.03.030).
[24] Z.A. Jahangirli, et al., J. Vac. Sci. Technol. 37(6), 062910 (2019) (https://doi.org/10.1116/1.5122702).
[25] I.I. Klimovskikh, et al., npj Quantum Mater. 5, 54 (2020) (https://doi.org/10.1038/s41535-020-00255-9).
[26] D.A. Estyunin, et al., APL Materials 8, 021105 (2020) (https://doi.org/10.1063/1.5142846).

[27] E.N. Orujlu, New Mater., Comp. App. 4(1), 38 (2020).
[28] J.-Q. Yan, et al., Phys. Rev. B100(10), 104409 (2019) (https://doi.org/10.1103/PhysRevB.100.104409).
[29] L. Chen, et all, J. Mater. Sci. 55(29), 14292 (2020) (https://doi.org/10.1007/s10853-020-05005-7).
[30] T. Murakami, et al., Phys. Rev. B 100, 195103 (2019) (https://doi.org/10.1103/PhysRevB.100.195103).
[31] L. Zhou, et all, Phys. Rev. B 102, 085114 (2020) (https://doi.org/10.1103/PhysRevB.102.085114).
[32] G. Shi, et all, Chinese Phys. Lett. 37(4), 047301 (2020) (https://doi.org/10.1088/0256-307X/37/4/047301).
[33] N.Kh. Abrikosov, et al., Inorg. Mater. (USSR) 4, 1638 (1968).
[34] D. Mateika, J. Cryst. Growth 13-14, 698 (1972) (https://doi.org/10.1016/0022-0248(72)90544-1).
[35] F. Grønvold, et al., J. Chem. Thermodyn. 4(6), 795 (1972) (https://doi.org/10.1016/0021-9614(72)90001-8)
[36] N.H. Abrikosov, et al, Nauka (USSR), 220 1975 (in Russian).
[37] T.L. Anderson, H.B. Krause, Acta Cryst. B30, 1307 (1974) (https://doi.org/10.1107/S0567740874004729).

Е.Н. Оруйлу[1], З.С. Алієв[2,3], І.Р. Амірасланов[3], М.Б. Бабанли[1]

Фазова рівновага системи $MnTe$-Sb_2Te_3 та синтез новітньої тернарної шаруватої структури – $MnSb_4Te_7$

[1]Інститут каталізу та неорганічної хімії АзНАН, Баку, Азербайджан, elnur.oruclu@yahoo.com
[2]Азербайджанський державний університет нафти та промисловості, Баку, Азербайджан, ziyasaliev@gmail.com
[3]Інститут фізики АзНАН, Баку, Азербайджан, iamiraslan@gmail.com

За допомогою методів диференціального термічного аналізу (DTA) та порошкової рентгенівської дифракції (PXRD), вперше побудовано фазову діаграму системи $MnTe$-Sb_2Te_3 у всьому діапазоні сполуки. Система містить дві потрійні шаруваті сполуки ван дер Ваальса (vdW). Окрім відомої $MnSb_2Te_4$, в системі знайдено нову сполуку $MnSb_4Te_7$, яка є структурним аналогом відомої $MnBi_4Te_7$. Параметри кристалічної структури обох сполук визначали уточненим методом Рітвельда, використовуючи підхід до фундаментальних параметрів. Встановлено, що обидві сполуки розкладаються в результаті перитектичних реакцій і мають значні діапазони однорідності. Назва системи також характеризується існуванням широкого кола твердого розчину на основі вихідного Sb_2Te_3. Отримані результати можуть бути корисними для росту монокристалів обох сполук з рідкої фази шляхом визначення площ первинної кристалізації.

Ключові слова: система $MnTe$-Sb_2Te_3; марганець сурми телуриди; магнітно-топологічні ізолятори; дифракція рентгенівських променів; фазова діаграма.